KUNGL TEKNISKA HÖGSKOLAN
Royal Institute of Technology

Interference Estimation in a Multicellular OFDMA Environment

JEREMY LAINÉ

RADIO COMMUNICATION SYSTEMS LABORATORY

KUNGL TEKNISKA HÖGSKOLAN
Royal Institute of Technology

Interference Estimation in a Multicellular OFDMA Environment

JEREMY LAINÉ

Master Thesis

July 2004

TRITA—S3—RST—0409
ISSN 1400—9137
ISRN KTH/RST/R--04/09--SE

RADIO COMMUNICATION SYSTEMS LABORATORY
DEPARTMENT OF SIGNALS, SENSORS AND SYSTEMS

Abstract

Orthogonal Frequency Division Multiple Access (OFDMA) is a multiple access technique that is starting to be examined as an alternative to Code Division Multiple Access (CDMA) for third generation cellular mobile systems. Until recently, OFDMA had received little attention for multicellular applications and as a consequence of this, few results are available on the impact of interference on OFDMA communications.

In this thesis, we study the behaviour of an OFDMA system with respect to the inter-cell interference. We show that due to the heterogeneous nature of the interference, interference estimation combined with soft-input channel decoders can be used to improve the performance of the system. We evaluate the performance gains obtained for different interference estimation techniques and show by means of realistic simulations that a low complexity algorithm can be used to achieve gains of up to 2dB.

This page intentionally contains only this sentence.

Acknowledgements

First of all I would like to thank Dominique Lacroix-Penther for making it possible for me to write my Master Thesis as part of her team at France Telecom R&D in Rennes, France. The team's vast experience in the field of digital communications and the warm welcome I received made for a most pleasant working environment.

I would especially like to thank Olivier Seller and Jean-Philippe Javaudin for their time, their advice and their valuable insights. Many of the ideas developed in this thesis were either inspired by or the direct product of the discussions we had.

I would also like to thank professor Slimane Ben Slimane at KTH, Stockholm. I am greatly indebted to him for his enlightening lectures and for supervising my thesis.

I would like to extend a warm thank you to my family for their unwavering support and encouragements throughout my studies, I could not have done it without you.

Finally, I would like to thank Claire for making me feel like the happiest person on earth every single day that goes by. Claire, this thesis is dedicated to you.

This page intentionally contains only this sentence.

Contents

List of Figures

This page intentionally contains only this sentence.

Chapter 1

Introduction

1.1 General background

Orthogonal Frequency Division Multiplexing (OFDM) is a multiple carrier technique that has proved to be very robust for communications over fading channels. In OFDM, the information to be transmitted is mapped onto several parallel sub-carriers which are chosen so that they are orthogonal to each other. Additionally, a guard interval is added to each OFDM symbol in order to combat the transmission channel's delay spread. In practical implementations, OFDM modulation is performed with an Inverse Fast Fourier Transform (IFFT) and demodulation with a Fast Fourier Transform (FFT).

When multiple access is desired, OFDM can be combined with Frequency Division Multiple Access (FDMA) or Time Division Multiple Access (TDMA) or a mix of both. The resulting scheme is called Orthogonal Frequency Division Multiple Access (OFDMA) and it is currently being examined for Third Generation (3G) or Beyond 3G mobile systems. In the rest of this document, OFDMA will in fact refer to Frequency Hopping OFDMA. In this multiple access technique, the users within a given cell are allocated a number of sub-carriers during one OFDM symbol, and the sub-carrier allocation changes at the next symbol interval.

Co-channel interference results from multiple users transmitting simultaneously on overlapping frequency bands. In the downlink of an OFDMA system, such interference is limited to inter-cell interference, as users within a given cell use sub-carriers which are orthogonal to each other. The Signal to Interference Ratio (SIR) is a metric that is commonly used to characterise the quality of a link.

1.2 Related work and specificity of OFDMA interference

1.2.1 Related work on SIR estimation

Over the years Code Division Multiple Access (CDMA), both in its single carrier and multiple carrier form (MC-CDMA) has been the object of numerous studies both in the academic and industrial world. As a consequence of this, there are many available publications dealing with the problem of SIR estimation for CDMA systems. These estimation methods are very specific to CDMA transmissions. For instance, the method developed in [1] exploits the subspace structure an observation vector to derive the SIR.

On the other hand, OFDMA has until now received relatively little attention, especially in multicellular environments. As a result of this, few results are available on the effect of inter-cell interference in OFDMA systems and SIR estimation is a new domain. One group currently focusing on multicellular interference in OFDMA systems is the "OFDM Study Item" [2] of the 3GPP/RAN1 standardisation group. In [3, 4], some simulation results (bit and block error rate measurements) were presented with a single interfering cell, but no actual interference estimation was attempted.

1.2.2 Specificity of OFDMA interference

In CDMA, the interference experienced by a user is homogeneous over time as long as no new users are admitted into or leave the system. Interference between users is directly related to the cross-correlation between their spreading codes. These codes are chosen so as to be orthogonal, or at least exhibit a low cross-correlation, and as a result of this techniques such as successive interference cancellation give good results. Furthermore, when no interference cancellation is attempted, the interference can be considered as noise.

The interference we experience in an OFDMA system is quite different from that of a CDMA system. When users from different cells are present on the same sub-carrier during a given OFDM symbol interval, what we have is directly a superposition of QPSK or QAM modulated signals with unknown fading gains. The methods presented in [5] and [6] have a wide application scope, but they are not practical in the OFDMA scenario. Indeed, not only do we not know the symbols and fading gains of the interfering users, we are also uncertain as to which time-frequency units the interfering users are present on. Trying to estimate all of these parameters would mean a prohibitively high computational cost.

1.3 Motivation and problem formulation

1.3.1 Motivation

Using OFDMA in an interference-limited environment is relatively new, as until now OFDMA was mostly used in non-cellular applications which where resource-limited. It is therefore desirable to obtain a better knowledge of how OFDMA systems perform in the presence of interference.

Soft-input channel decoders such as turbocode decoders [7] are decoders that are operate on soft-valued reliability metrics, such as log-likelihood ratios (LLR). Supposing we have access to information about the interference that corrupted the signal during transmission, and the variation of this interference over time, it is possible to adjust the metrics that are fed to the decoder to reflect the fact that certain symbols are more reliable than others. It has been shown in [3, 4] that adjusting the decision metrics based on perfect knowledge of the instantaneous SIR results in considerable performance improvements in terms of Bit Error Rates (BER) and Block Error Rates (BLER).

1.3.2 Problem formulation

The first goal of the present thesis is to establish, by means of simulations, how an OFDMA system behaves in the presence of realistic inter-cell interference. The second

goal is to propose an interference estimation method for such a system in order to adjust the likelihood metrics that are fed to the channel decoder.

Decoding the interfering signals and performing interference subtraction are outside the scope of the present study. Channel estimation is also outside the scope of the present study.

1.4 Thesis outline

We start by presenting the system that is to be studied along with the assumptions that were made in Chapter 2. In Chapter 3 we derive some general results concerning the effect of interference on transmissions and show that averaging interference to make it similar to noise is not necessarily desirable. In Chapter 4 we show how interference estimation can improve the performance of a soft channel decoder and describe the interference estimation techniques that we examined. In Chapter 5 we describe the simulation chain that was developed and evaluate the performance of different interference estimation techniques. In Chapter 6 we summarise the conclusions of this study and give some ideas for future work.

This page intentionally contains only this sentence.

Chapter 2

Context and system models

2.1 Context and scenario

In order to produce results which are as relevant as possible for real-word applications, it was decided that the current study would be based on the OFDMA system defined by the "OFDM Study Item" of the 3GPP/RAN1 working group, namely an OFDM enhancement of the High Speed Downlink Packet Access of UMTS Release 5.

2.1.1 Third generation systems, UMTS and 3GPP

The 3rd Generation Partnership Project (3GPP) is a collaboration that was started in 1998 and is responsible of the technical specifications for the Universal Mobile Telecommunication System (UMTS). The technical specifications work is accomplished by five Technical Specification Groups (TSG), each of which focuses on one aspect of UMTS. The TSG Radio Access Network (TSG RAN) is responsible for the Universal Terrestrial Radio Access Network (UTRAN).

2.1.2 An OFDM enhancement of HSDPA

Prior to Release 5, UMTS specifications defined a Wideband CDMA (WCDMA) system with a maximum data rate of 2Mbps. For applications such as multimedia services, there is a need for higher data rates. In Release 5 of the UMTS specifications, the High Speed Data Packet Access (HSDPA) [8, 9] was introduced to meet this demand for increased bandwidth. By making use of fast link adaptation, fast hybrid automatic repeat request and fast scheduling, HSDPA provides peak data rates of 8-10 Mbps.

In its current specification, UMTS (and hence HSDPA) uses Wideband CDMA for multiple access. CDMA, which is a spread spectrum technique, was chosen mainly because it enables a flexible multicellular deployment with full frequency reuse. Furthermore, CDMA has been extensively studied in real-life situations such as IS-95 networks. An alternative to CDMA is to use Orthogonal Frequency Division Multiple Access (OFDMA). The goal of the "OFDM Study Item" [2] of TSG RAN1 is precisely to evaluate the feasibility and benefits of introducing OFDM to UTRAN.

2.2 System description and parameters

2.2.1 Overview

In this study, we examine the downlink of a multicellular OFDMA system. The reuse factor is of one, meaning that all the cells present in the network use the same frequency band. If we consider the users of a given cell, they will receive both the desired signal and interference from neighbouring cells in the same frequency band, as illustrated in Figure 2.1.

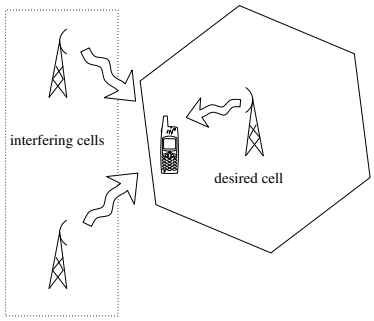

Figure 2.1: multicellular environment experienced by each user

In each cell, a base station or Node B in UMTS terminology serves up to 15 users. Signalling is not the object of the present study so we will only consider the transmission of the users' data. The data to be transmitted by each user is coded, interleaved and passed to a mapping unit which uses either QPSK or 16-QAM modulation. The traffic for the different users is then multiplexed using a time-frequency mapping that is detailed in section 2.2.2. The multiplexed traffic then undergoes OFDM modulation, which involves inserting unused carriers on either side of the data-bearing carriers, performing an Inverse Fast Fourier Transform and adding a cyclic prefix. These operations are summarised in Figure 5.1. For a more detailed description of the system's transmission and reception chains please refer to section 5.1.1.

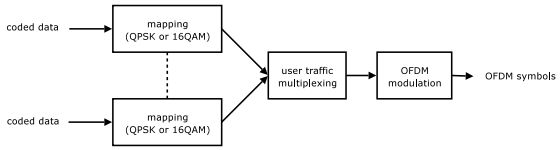

Figure 2.2: overview of OFDMA transmission

2.2.2 Frames and user traffic multiplexing

The basic time interval we consider in the present study is an HS-DSCH sub-frame, which corresponds to 12 OFDM symbols. From here on, we will simply refer to these as *frames*. The frames have a duration of 2ms and this duration is often referred to as a Transmission Time Interval (TTI).

The OFDM frequency band is divided into 15 sub-bands, that is to say blocks of consecutive sub-carriers. One such sub-band during one OFDM symbol interval is referred to as an *OFDM unit*. User traffic is multiplexed by allocating one OFDM unit to each active user at each symbol interval. The patterns used to multiplex the traffic of different users within a given cell need to be orthogonal in order to avoid intra-cell interference. To allow full frequency reuse without resource planning, the time-frequency mappings should also minimise inter-cell interference.

The time-frequency (T-F) mapping that is used is based on a truncated Costas sequence of length 15 [10]. Costas arrays are $n \times n$ arrays consisting of dots and blanks with exactly one dot in each row and column. These arrays were first studied for radar applications as the two dimensional patterns they represent in the time-frequency plane have an optimum ambiguity function.

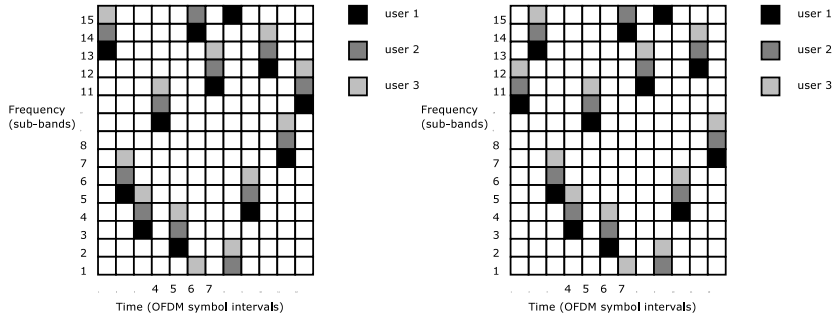

(a) allocation pattern 1

(b) allocation pattern 2

Figure 2.3: 2 sets of time-frequency allocation patterns

For a given cell and TTI, the allocation patterns for the different users are obtained as a cyclic frequency shift of the basic allocation pattern. The frequency shift is an integer number of sub-bands. Different sets of T-F allocation patterns can be obtained through a cyclic time shift of an integer number of OFDM symbol intervals. To illustrate this, two sets of time-frequency allocation patterns are represented in Figure 2.3. The right-hand set is obtained by shifting the left-hand set by one OFDM symbol duration.

Every TTI, each cell selects a set of allocation patterns at random, which corresponds to drawing a random time-shift. There are 12 possible sets of T-F allocation patterns, each of which contains 15 allocation patterns.

2.2.3 Link-level parameters

The link-level parameters of the system are those described as the parameter set 2 in [2]. They are summarised in the following table.

Parameter	Value
Carrier frequency	2GHz
Channel width	5MHz
Channel type	AWGN or ITU Vehicular A 30km/h
TTI	2ms
FFT size	1024
Modulated carriers	705
Guard interval	64
OFDM bandwidth	4.495MHz
Turbocoder	UMTS-like, max 6 iterations

Data is modulated using either QPSK or 16-QAM, and this modulation is not changed during transmissions as link adaptation is not the object of the present study. Furthermore, in order to limit the number of possible configurations, only one coding rate was examined per type of modulation.

Modulation	QPSK	16QAM
Coding rate	2/3	1/2
Information block size	752 bits	1128 bits

2.3 Assumptions

2.3.1 Channel knowledge

In the present study, equalisation is done with ideal knowledge of the channel. In a real implementation, channel estimation would most likely be achieved with the help of pilot sub-carriers. This was not attempted for two reasons. The first reason is that inserting pilot sub-carriers would complicate the multiplexing and demultiplexing of the user traffic. The second reason is that channel estimation in the presence of inter-cell interference is not a trivial task and would best be handled in a separate study.

2.3.2 Interfering cells, synchronisation

The scenario that was used in most of the simulations was one cell of interest and two interfering cells. The transmitters of all the cells are assumed to be synchronised in frequency, which is a reasonable assumption since base stations use high-quality oscillators. Unless specified otherwise, the interfering signals are assumed to be received with a random delay of up to one OFDM symbol relative to the signal of interest. Due to the multiplexing scheme that is used, it is not necessary to consider a delay of more than one OFDM symbol since a delay of an integer number of OFDM symbols corresponds to using a different set of T-F allocation patterns. As the pattern set is chosen at random for each cell, we explore all the possible combinations.

Chapter 3

Transmissions in the presence of interference

3.1 Bit error rates for uncoded transmissions with noise and interference

In this section, we assume that both a desired signal and an interfering signal are transmitted over an Additive White Gaussian Noise (AWGN) channel with no channel coding and we determine the resulting bit error rate. The interferer uses the same modulation as the desired signal and is assumed to have a random phase. The desired signal has symbol energy S, the interfering signal has symbol energy I and the noise power is N.

3.1.1 QPSK modulation

Let us consider the case where the signal uses a QPSK modulation and a Gray mapping with normalised symbol energy. Due to the problem's symmetry, the bit error probability P_e is the same for the different bits. Denoting z the real component of the noise, the error probability for the first bit b_1 becomes

$$P_e = Pr(b_1 \neq 0 \mid b_1 = 0) = \int_0^{2\pi} Pr\left(\sqrt{\frac{S}{2}} + \sqrt{I}\cos\theta + z < 0\right) d\theta$$

and as z is a real-valued Gaussian random variable with variance $\frac{N}{2}$ this yields

$$P_e = \int_0^{2\pi} Q\left(\frac{\sqrt{S} + \sqrt{2I}\cos\theta}{\sqrt{N}}\right) d\theta$$

With this expression, we are able to calculate the bit error rate for different values of the Signal to Noise Ratio (SNR) and Signal to Interference Ratio (SIR). In Figure 3.1, the bit error rate for different SIR levels is plotted as a function of the SNR. Each plot corresponds to a fixed SIR value, with the 100dB curve serving as a reference since it represents the case with noise only. Similar plots are often used to illustrate the fact that with a large number of interferers, the interference can be considered as Gaussian due to the central limit theorem and hence we encounter an error floor which is fixed

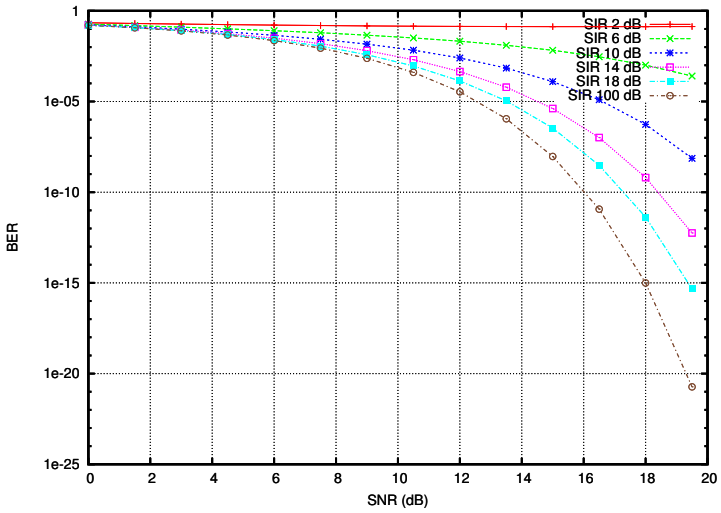

Figure 3.1: BER vs SNR for uncoded QPSK with one interferer on AWGN

by the SIR level. In the present case we consider a single interferer and no such error floor is apparent.

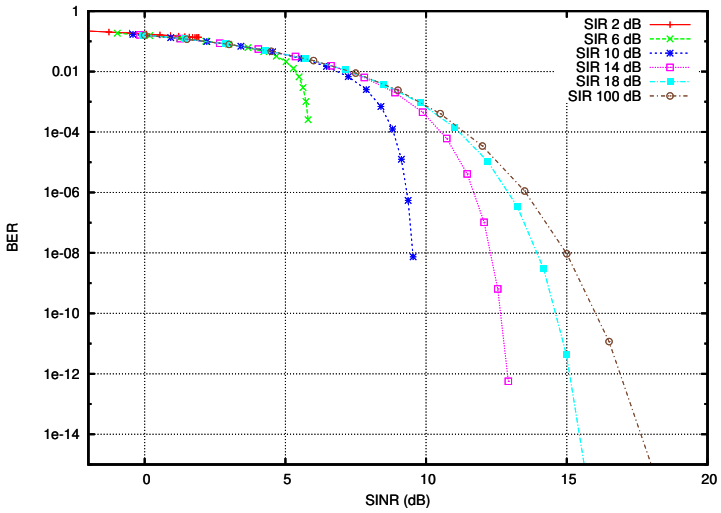

Figure 3.2: BER vs SINR for uncoded QPSK with one interferer on AWGN

In Figure 3.2, the bit error rate is plotted as a function of the Signal to Interference plus Noise Ratio (SINR). It is interesting to note that the curves are superimposed for low SINR values (or equivalently low SNR since for each curve the SIR is constant) but then diverge as the SINR increases, which indicates that the noise and the interference are not equivalent.

3.1.2 16-QAM modulation

For 16-QAM, deriving a closed-form expression of the bit error probability is tedious, so we instead obtain BER measurements by means of simulations. A plot of the bit error rate versus the SINR is presented in Figure 3.3. We can see that in the case of 16-QAM, the curves all lie close to the noise-only plot, indicating that the 16-QAM interference is more akin to noise than QPSK interference. This can be explained by the fact that unlike QPSK interference, 16-QAM interference does not have a constant amplitude. Bearing in mind that a random phase was assumed, the two dimensional probability density function (PDF) for a 16-QAM signal (3 concentric rings) is closer to a 2-dimensional Gaussian PDF than the PDF for a QPSK signal (a single ring).

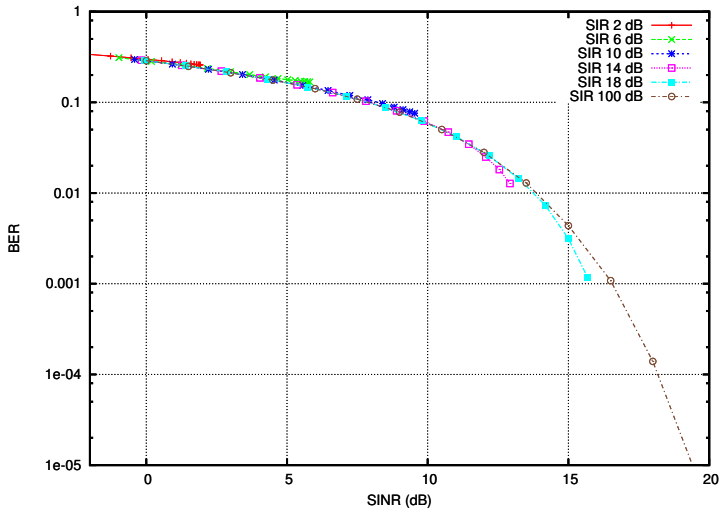

Figure 3.3: BER vs SINR for uncoded 16-QAM with one interferer on AWGN

3.2 Mutual information for transmissions with interference and noise

In order to get a measurement of the quantity of information that can be transmitted without error over an AWGN channel with interference, we can look at the average mutual information between the channel input and the channel output. The channel input X is a discrete random variable whose possible outcomes are taken from either a QPSK or a 16-QAM constellation, while the channel output Y is a continuous random variable. The average mutual information information between X and Y is defined as

$$I(X;Y) = \sum_{i=1}^{N} \int_{-\infty}^{\infty} p(y \mid x_i) P(x_i) \log \frac{p(y \mid x_i)}{p(y)} dy$$

In order to obtain numerical values of this average mutual information for different values of the SIR and the SNR, we sample the signal space and use the fact that summing random variables translates into performing a convolution on their probability density functions.

3.2.1 Interferer present all the time

The plots in Figure 3.4 represent the average mutual information when a single interferer is transmitting all the time. We can see from the curves that the noise and the interference are not equivalent. For a given interference plus noise level, the more interference dominates noise, the more information can be transmitted.

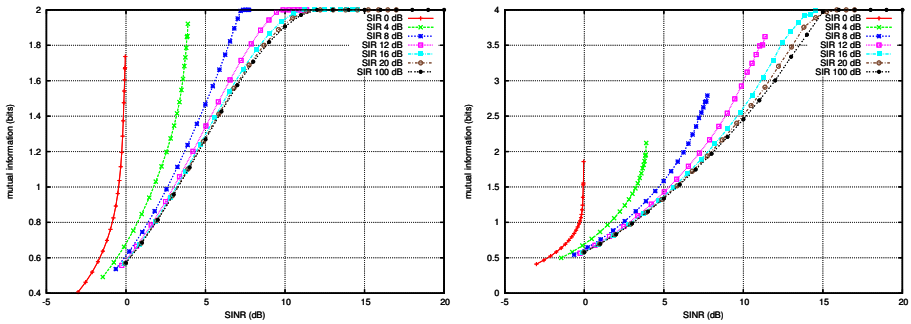

(a) QPSK signal and interference

(b) 16-QAM signal and interference

Figure 3.4: mutual information with one interferer on AWGN

3.2.2 Interferer present part of the time

It is also interesting to consider the case when an interferer is present only part of the time. Indeed, in the OFDMA scenario that is considered for this study, user traffic is mapped onto OFDM units using a different pattern for each cell. As a result of this, if adjacent cells are not running at full load, at times certain sub-carriers will be free of interference. The plots in Figure 3.5 represent the average mutual information when an interferer is present only 1/3 of the time. The SIR mentioned on the plots is actually the average SIR since the interference is bursty.

We observe the same behaviour as when the interferer is present all of the time. In conclusion, whether the interferer is present all or only part of the time, we can see that at equivalent power levels non-Gaussian interference leads to a higher mutual information than Gaussian interference. This is interesting because CDMA and OFDMA do not average the interference at the same level. CDMA averages interference at the symbol level which makes it Gaussian whereas OFDMA averages interference at the block level preserving its bursty and non-Gaussian nature at the symbol level.

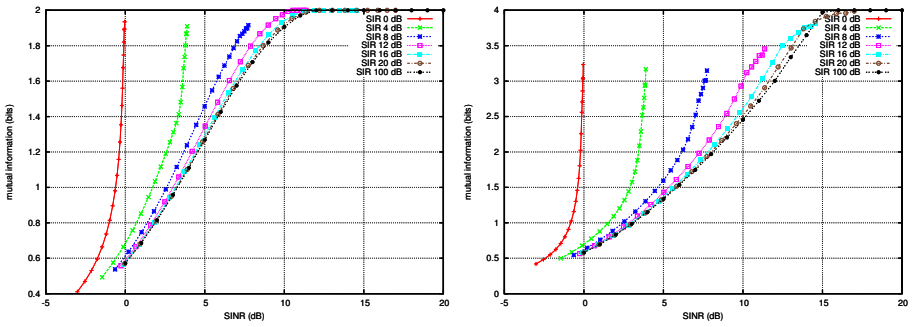

(a) QPSK signal and interference

(b) 16-QAM signal and interference

Figure 3.5: mutual information with one interferer (probability 1/3) on AWGN

This page intentionally contains only this sentence.

Chapter 4

Interference estimation

4.1 Log-likelihood ratios and interference

4.1.1 Log-likelihood ratios

In a communications system, the role of the channel decoder is to decide what signal transmitted based on the observation of the received signal. A common rule for making this decision is the maximum *a posteriori* rule (MAP). Let x denote a signal from a discrete signal set $\{s_1, \ldots, s_N\}$ that is transmitted and r be the received signal. According to Bayes rule, the *a posteriori* probability $P(x = s_i \mid r)$ can be written as

$$P(x = s_i \mid r) = \frac{p(r \mid x = s_i) P(x = s_i)}{p(x)}$$

Making a decision based on the MAP rule means finding the element i of the signal set that maximises the *a posteriori* probability. In the case of binary signalling using a signal set $\{s_1, s_2\}$, the criterion for deciding whether s_1 or s_2 was transmitted is to look at which of $P(x = s_1 \mid r)$ or $P(x = s_2 \mid r)$ is greatest. An equivalent formulation is to examine whether the likelihood ratio $\Lambda(r)$ is greater or lesser than 1, with the likelihood ratio defined as

$$\Lambda(r) = \frac{P(x = s_1 \mid r)}{P(x = s_2 \mid r)} = \frac{p(r \mid x = s_1) P(x = s_1)}{p(r \mid x = s_2) P(x = s_2)} \tag{4.1}$$

If we take the log of 4.1, we obtain the log-likelihood ratio (LLR)

$$L(x \mid r) = \ln\left(\frac{p(r \mid x = s_1)}{p(r \mid x = s_2)}\right) + \ln\left(\frac{P(x = s_1)}{P(x = s_2)}\right) \tag{4.2}$$

In the case where s_1 and s_2 are transmitted with equal probabilities, the second term of the above expression is zero.

4.1.2 LLRs on flat fading channels with AWGN

Let us consider the case where a signal is transmitted using antipodal signalling over a flat fading channel with additive white Gaussian noise. The received signal can be expressed as a function of the transmitted signal x, the channel coefficient h and the noise n which is a Gaussian random variable with variance σ^2 as

$$r = hx + n, \quad x \in \left\{ +\sqrt{E_b}, -\sqrt{E_b} \right\}$$

If we furthermore consider equal *a priori* probabilities for the two possible signals $+\sqrt{E_b}$ and $-\sqrt{E_b}$, using the fact that n is a Gaussian random variable, the log-likelihood ratio can written as

$$\begin{aligned} L(x \mid r) &= \ln\left(\frac{p(r|h,x=+\sqrt{E_b})}{p(r|h,x=-\sqrt{E_b})}\right) \\ &= \ln\left(\frac{\exp\left(-\frac{|r-h\sqrt{E_b}|^2}{2\sigma^2}\right)}{\exp\left(-\frac{|r+h\sqrt{E_b}|^2}{2\sigma^2}\right)}\right) \end{aligned}$$

which can be simplified into

$$L(x \mid r) = 2\frac{\sqrt{E_b}}{\sigma^2}\Re\left(h^* r\right) \tag{4.3}$$

Equation 4.3 is interesting as it illustrates the fact that knowledge of the signal to noise ratio is needed in order to compute the log-likelihood ratio. It also shows that the signal to noise ratio $\frac{\sqrt{E_b}}{2\sigma^2}$ appears as a multiplicative term in the LLR.

4.1.3 Adjusting LLRs for interference

In the previous section, we derived an expression of the LLR in the case of transmissions over slow, frequency non-selective fading channels in the presence of additive white Gaussian noise. In this section we examine how the metrics that are output by the demodulation stage can be adjusted to take into account the presence of inter-cellular interference.

First of all, it should be noted that the hypothesis of a flat fading channel holds in the OFDMA system we are studying as the goal of OFDM is precisely to transform a frequency-selective channel into multiple narrow flat fading sub-channels. However, in a multicellular environment, it is no longer reasonable to suppose that the interference is Gaussian and white. Deriving an exact expression of the LLR for a given sub-band and time slot using formula 4.2 would require knowledge of the number of interferers present and their respective phases and amplitudes. Such detailed information is unfortunately not usually available, but will assume that information about the total interference power can be obtained by some means.

Let us denote LLR_{in} the metrics output by the demodulator based on formula 4.3. These metrics are not the actual log-likelihood ratio as they only take into account the estimate of the noise level that was given to the demodulator. In order for the channel decoder to produce better decisions, we should feed it metrics which we will denote LLR_{out} which are closer to the true LLR. If we denote N the noise power and I the interference power, our goal is to identify a function f such that

$$LLR_{out} = f\left(LLR_{in}, I, N\right)$$

is a better estimation of the log-likelihood ratio.

Simple I+N method A simple LLR weighting method is to consider that the interference will have an impact which is similar to the Gaussian noise, and hence use

$$LLR_{out} = LLR_{in}\frac{N}{I+N} \tag{4.4}$$

Equivalent SNR mapping Another method that was examined is to use a mapping of (SIR,SNR) to an equivalent SNR in terms of Bit Error Rates (BER). Such a mapping was produced based on the results of section 3.1. We calculated the BER for uncoded transmissions over an AWGN channel in the presence of interference for different (SIR,SNR) points. For each one of these points, we then looked up the SNR level for a noise-only situation which yielded the same BER. If we call N_{eq} the mapping function thus constructed, the LLR will be adjusted as

$$LLR_{out} = LLR_{in}\frac{N}{N_{eq}(I,N)} \tag{4.5}$$

4.2 Interference estimation methods

4.2.1 Ideal estimation

In order to obtain an upper bound on the performance one can expect by performing LLR weighting based on the interference level, several simulations were performed using perfect interference estimation. That is to say that for every sub-carrier of each OFDM symbol we have the exact powers of both the noise and the inter-cell interference.

4.2.2 Interferer location

The first practical interference estimation method that was examined relies on the fact that in order to avoid creating excessive interference in the neighbouring cells, a cell will not operate at full load. As a consequence of this, in certain time-frequency (T-F) units the cell of interest does not transmit and we have only interference. We will refer to these T-F units as the *observable T-F units*. In this section, it is assumed that the cell of interest is synchronised in time and frequency with the interfering cells.

The allocation pattern for the users in the interfering cells can be viewed as a repetition code. This means that estimating in which T-F units the interferers are present can be viewed as block-decoding a repetition code with a certain number of erasures, namely the T-F units where our cell of interest is present. This is not strictly true as we in fact have a superposition of several interfering cells, but a certain amount of information can possibly still be recovered by analysing the power levels in the *observable T-F units*.

We developed an algorithm that iteratively tries to detect the set of allocation patterns, the number of active users and a power measurement for the strongest interfering cell. The motivation for constructing an iterative algorithm as opposed to one that detects all the interferers in one pass is that the sets of T-F allocation patterns are not orthogonal to each other. This means that a given observation of the interference-only units cannot be decomposed into a unique superposition of interfering pattern sets, cell loads and powers.

The algorithm is initialised with the knowledge of the allocation set and number of users for the cell of interest. From this it determines which time-frequency units are *observable T-F units*. Each iteration of the algorithm can be summarised as follows:

1. For each possible user u of each available allocation pattern set s, compute the average power $P(s,u)$ in the *observable T-F units* where the user would have transmitted.
2. From the $P(s,u)$ metrics determine the allocation set and number of users of the strongest interfering cell.
3. Estimate the power contribution of the detected cell and subtract its contribution from the powers in the *observable T-F units*.

The algorithm stops when it reaches a specified maximum number of iterations or when it is unable to locate an additional cell, whichever comes first. From the detected metrics, it then produces an estimate of the total interference power in the T-F units where the cell of interest is active. For this step, two modes of operation were considered. The difference between these two modes is the power which is considered for each interfering cell's contribution. In the first mode, for each interfering cell we use one power estimate per sub-band over the whole frame duration. In the second mode, for each interfering cell we use an averaged power over all the T-F units where the interferer is present.

4.2.3 Demapping and remapping

Another estimation technique that was examined is to calculate the difference between the received signal and the closest constellation point multiplied by the estimate of the channel. This is achieved by demapping the received signal, taking a hard decision and remapping the estimated symbol.

For a given time t let x_t denote the constellation point that was transmitted on a given sub-carrier by the cell of interest, h_t the corresponding channel coefficient and i_t the total interference for at time t. The received signal r_t can be written as

$$r_t = h_t x_t + i_t$$

If we call $\hat{x_t}$ the estimated mapped symbol and $\hat{h_t}$ the estimate of the channel coefficient, our estimate of the total interference for the considered sub-carrier is

$$\hat{i_t} = r_t - \hat{h_t}\hat{x_t}$$

The estimated mapped symbol $\hat{x_t}$ is the constellation point that minimises $\left\| r_t - \hat{h_t}\hat{x_t} \right\|$. As x_t is one of the constellation points, we have the following relationship

$$\left\| r_t - \hat{h_t}\hat{x_t} \right\| \leq \left\| r_t - \hat{h_t}x_t \right\|$$

In the case where $\hat{h_t} = h_t$, that is when our estimate of the channel is correct, the above relationship becomes

$$\left\| \hat{i_t} \right\| \leq \| i_t \|$$

This means that if we have a perfect estimate of the channel, the estimate of the interference will always have a power that is lower or equal to the actual interference power. We will see later on that this is not necessarily a problem as we are more concerned about the relative interference powers for different parts of the signal than about the actual value of the interference power.

4.3 Filtering interference estimates

In section 2.2.2 we saw that user traffic is multiplexed by mapping user data onto OFDM units according to a time-frequency allocation pattern. Furthermore we saw that for each OFDM symbol duration, a given user is allocated a frequency sub-band, that is to say a block of consecutive carriers. If the cell of interest and the interfering cells are synchronised in time and frequency, for each sub-band of a given OFDM symbol the interference level will be constant. If however the interfering cells are not synchronised with the cell of interest, this is no longer true. Nevertheless, the interference experienced on adjacent sub-carriers will remain strongly correlated, and it is therefore reasonable to perform filtering of the interference estimates per sub-bands. One filtering we experimented with is a polynomial interpolation on the interference power estimates.

This page intentionally contains only this sentence.

Chapter 5

Simulation method and results

5.1 Simulation setup

We evaluated the performance of the different interference estimation and LLR weighting methods using link-level Monte Carlo simulations. To this end, a multicellular OFDM simulation chain was implemented using SystemC. An overview of this simulation chain is given in Figure 5.1. The simulator consists of one useful cell, a variable number of interfering cells and additional thermal noise. The multi cell environment is an extension of the work presented in [3, 4], where only one interfering cell was considered.

The simulation chain can be broken down into transmission and reception blocks for the cell of interest and some additional blocks which simulate the effects of the transmission channel, noise and the interfering cells. Both the useful and the interfering signals travel over independent channels which can be either a simple AWGN channel or an ITU Vehicular A (30km/h velocity) channel.

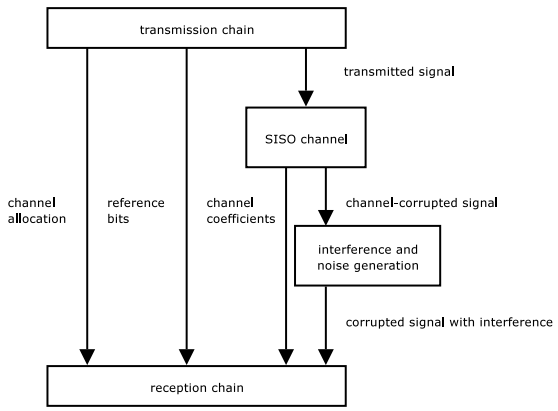

Figure 5.1: overview of the simulation chain

The Signal to Interference Ratio (SIR) and Signal to Noise Ratio (SNR) values are controlled by a combining block, which sums the useful signal, the interfering signals and the thermal noise, as illustrated in Figure 5.2. The combining block is also able to

introduce a random time and/or frequency shift between the signal of the cell of interest and the interfering cells.

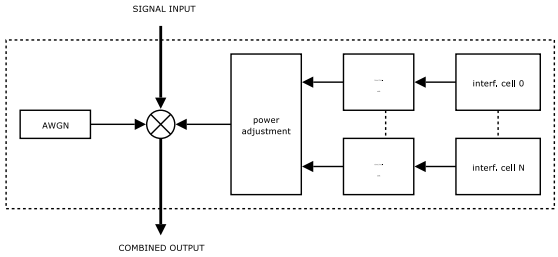

Figure 5.2: combining useful and interfering signals

5.1.1 Transmission and reception

The transmission and reception chains used for the cell of interest are illustrated in Figure 5.3. The shaded blocks are those directly concerned by the present study, namely the user traffic multiplexing/demultiplexing blocks and the interference estimation block.

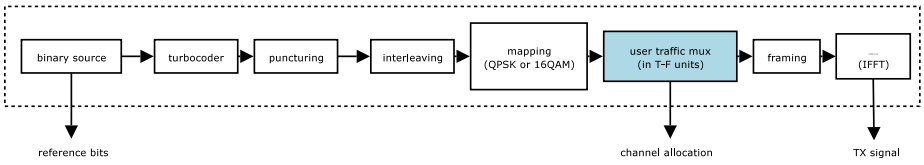

(a) transmission chain

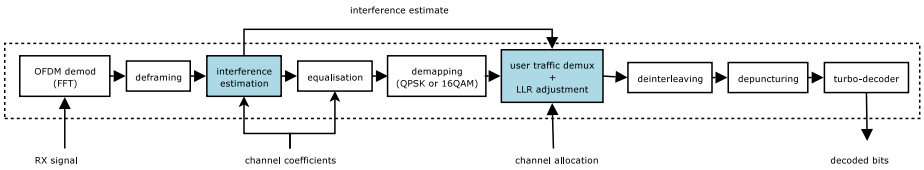

(b) reception chain

Figure 5.3: transmission and reception chains

5.1.2 SNR and SIR values

The simulation chain operates using an actual value interface, meaning that we control the actual SNR and SIR values for each frame. As we consider various loads both

for the cell of interest and the interfering cell, and the OFDM framing operation adds unmodulated carriers on either side of the available carriers, a word of explanation is needed as to what the SIR and SNR values represent.

The SNR represents the Signal to Interference Ratio in the used frequency band. If S represents the signal power for the cell of interest and N represents the total noise power, the SNR we consider is expressed as

$$SNR = \frac{S}{N} \times \frac{TotalSubBands}{UsedSubBands} \times \frac{FFTSize}{AvailableCarriers}$$

The SIR represents the ratio between the signal power S for the cell of interest and the total interfering power I, so that we have

$$SIR = \frac{S}{I}$$

5.2 Initial results on OFDM with interference

The results presented in this section were produced at an early stage of the study in order to assess the impact of interference on OFDM transmissions. The results also illustrate what performance gain can be obtained given full or an averaged knowledge of the interference. Some of these results were presented as part of the European Over-DRiVE project [11]. For all the simulations in this section, the channel model is an ITU Vehicular A 30km/h channel.

5.2.1 Impact of interference without knowledge of the interference

A first set of simulations was performed with a receiver that has no knowledge of the interference, that is to say that the receiver considers that only thermal noise is present. Simulations were run with the cell of interest at full load (15 users) and a single interfering cell at approximately half load (8 users). The interfering cell is unsynchronised with the cell of interest, there is a random delay of up to one OFDM symbol between the two cells.

The results are presented in terms of average Bit Error Rates (BER) and Block (frame) Error Rates (BLER). The variable used for the x axis is the Signal to Interference plus Noise Ratio (SINR). Results for QPSK modulation are plotted in Figures 5.4 and 5.5, those for 16-QAM are plotted in Figures 5.6 and 5.7. We can see that the error curves are not very dependant on the relative contributions of the noise and interference, the controlling variable is the SINR. This indicates that for this system, the interfering cell can be modelled quite accurately by additive noise.

Unlike W-CDMA systems, the interference experienced by a given user in the OFDMA system is not homogeneous. Because the interfering cell is not fully loaded, some of the time-frequency units are free of interference while others suffer from high interference levels. We can see that the system is able to average out this heterogeneous interference and make its impact similar to that of thermal noise. This behaviour can be attributed to the channel coding. It is a well known fact that OFDM transmissions need to be encoded in order to exploit frequency diversity, but here we find another justification for the use of Forward Error Correction (FEC).

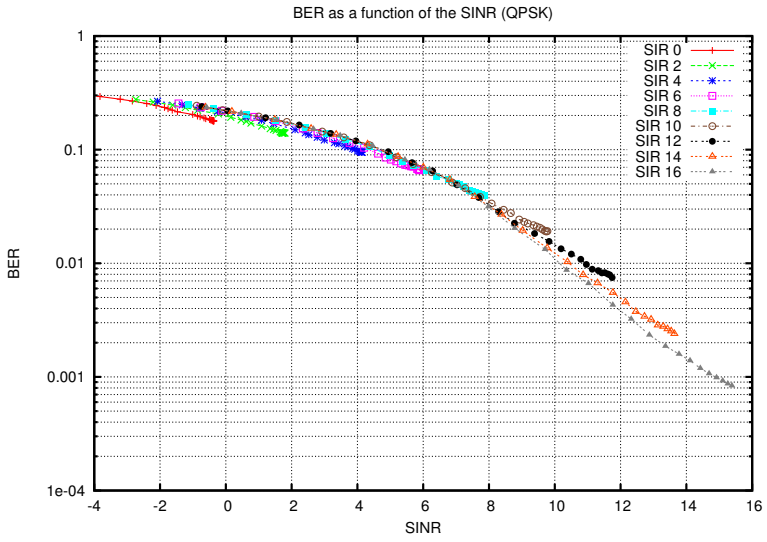

Figure 5.4: BER for QPSK in the presence of interference

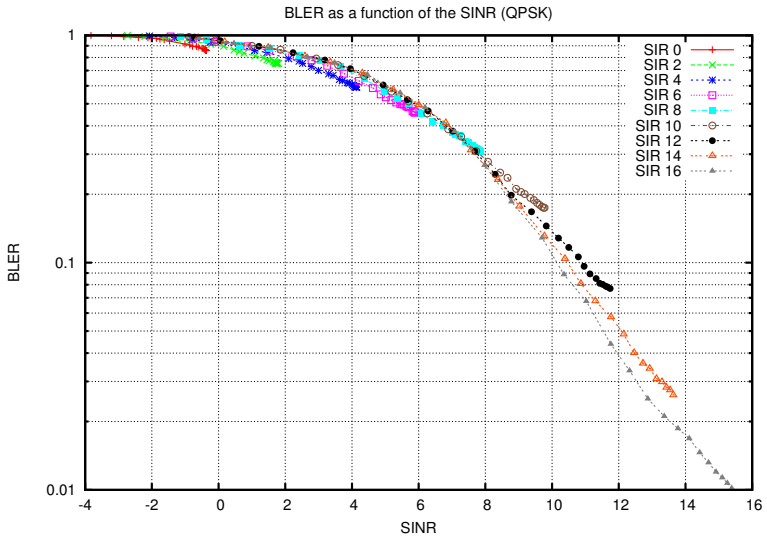

Figure 5.5: BLER for QPSK in the presence of interference

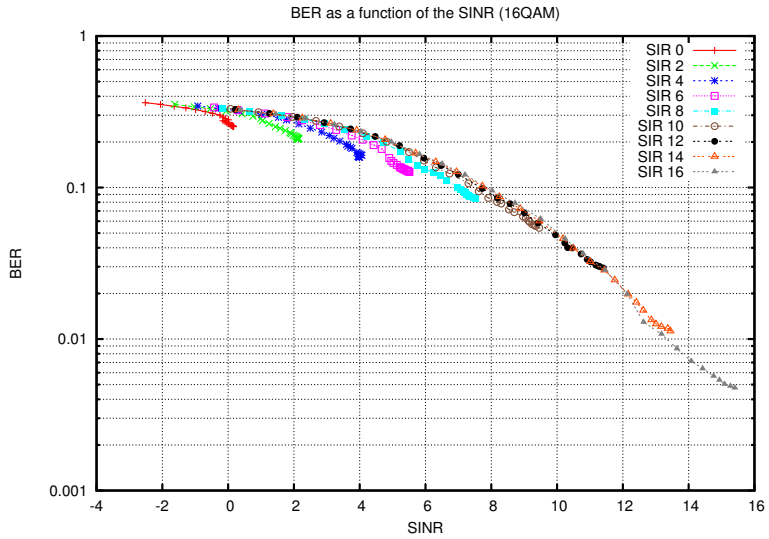

Figure 5.6: BER for 16QAM in the presence of interference

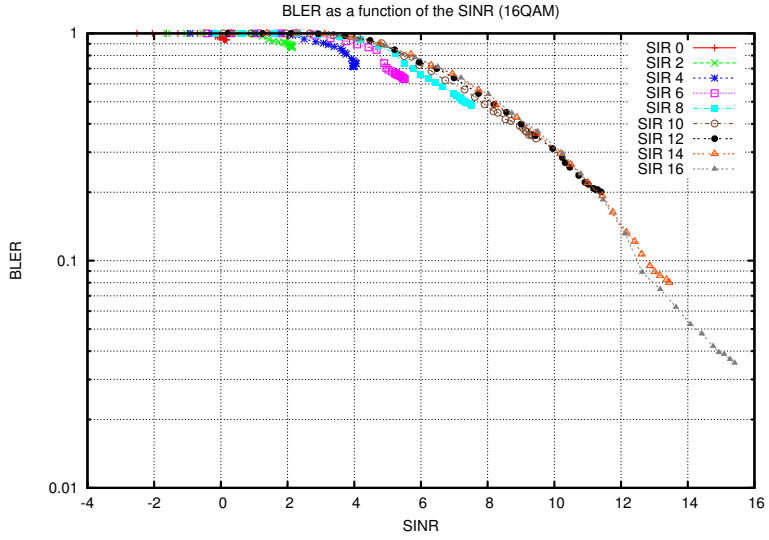

Figure 5.7: BLER for 16QAM in the presence of interference

5.2.2 With ideal knowledge of the interference

We saw in the previous section that without knowledge of the heterogeneous nature of the interference, the OFDM system can average out the interference, making its impact similar to that of noise. However, exploiting the fluctuations in the interference power to adjust the metrics fed to the channel decoder is likely to lead to performance gains. A second set of simulations was therefore conducted to gain an insight of what performance improvements can be expected in a multicellular environment given full knowledge of the interference.

For these simulations, two interfering cells are used with relative powers of 0 and -5dB. The cell of interest runs at full load, while the interfering cells are loaded with either 2, 5 or 8 users each. We also consider thermal noise at a fixed level of -15dB. The receiver is given full knowledge of the interfering power, that is to say that for each sub-carrier within a given OFDM symbol, the receiver has a measurement of the total interfering power. With this informations, the receiver performs LLR weighting using the $I+N$ method described in section 4.1.3.

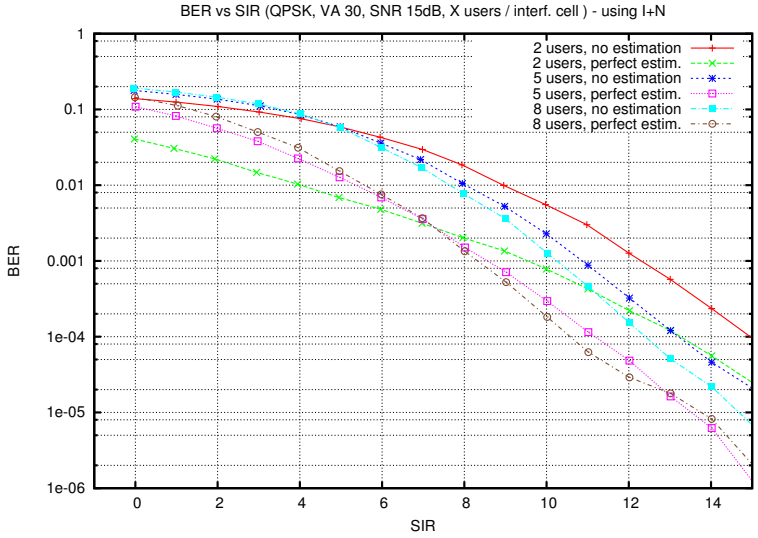

Figure 5.8: BER for QPSK : no estimation vs. ideal estimation

The performance is once again evaluated in terms of average bit error rate (BER) and block error rates (BLER). Figures 5.8 and 5.9 represent the results obtained for QPSK while Figures 5.10 and 5.11 represent those for 16-QAM modulation.

It is clear from the results that exploiting a measurement of the interference leads to a considerable performance improvement. The first thing we can observe is that the performance gain decreases as the SIR increases. This seems perfectly reasonable, since the thermal noise level is fixed, and as the SIR increases, the effect of the noise progressively dominates the effect of the interference.

We can also see that the performance gain is greatest when the interference is well localised, namely when the interfering cells have 2 active users each. This was to be expected, since our scheme works by weighting the bit likelihood metrics according to the interference. When the interference is received over a limited number of modulation

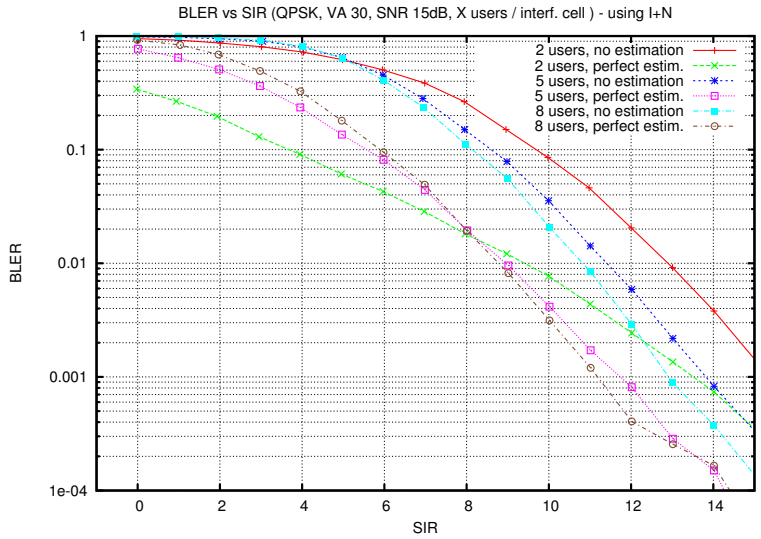

Figure 5.9: BLER for QPSK : no estimation vs. ideal estimation

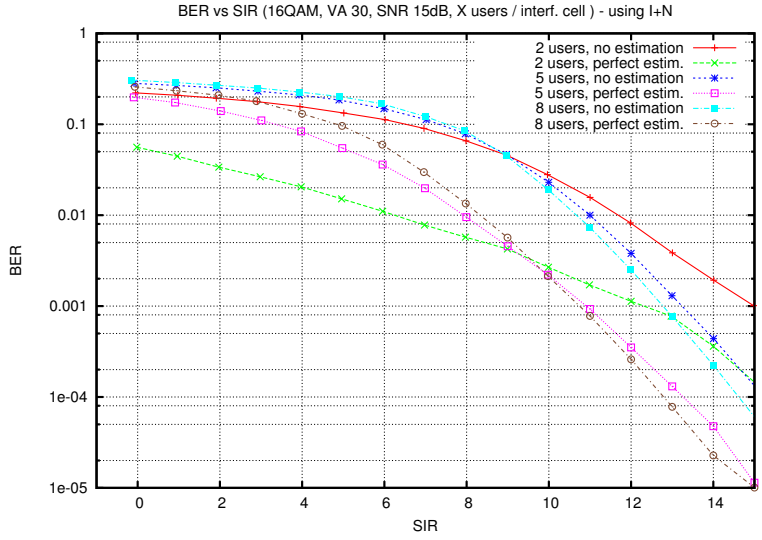

Figure 5.10: BER for 16-QAM : no estimation vs. ideal estimation

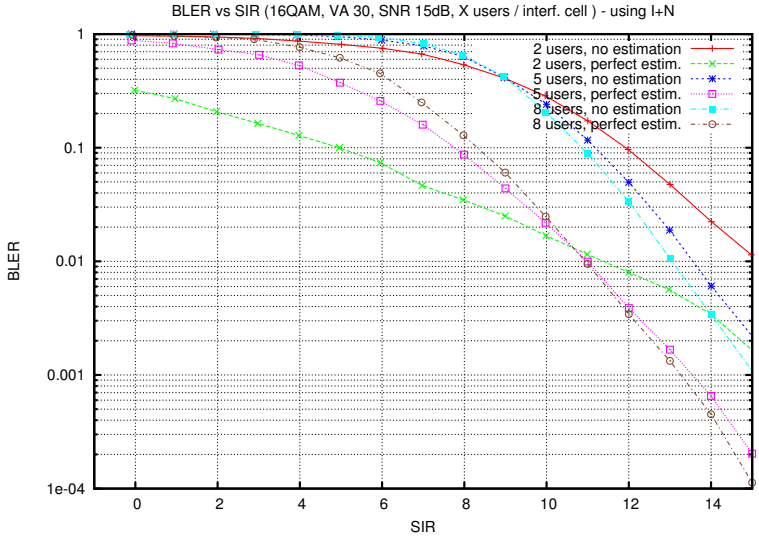

Figure 5.11: BLER for 16-QAM : no estimation vs. ideal estimation

units, these modulation units are marked as unreliable and the channel decoder will mainly base its decisions on the interference-free units.

The following table summarises the performance gain over no estimation for a BLER of 10^{-2} in the different configurations.

users per interfering cell	QPSK	16-QAM
2 users	3.2 dB	3.8 dB
5 users	2.6 dB	2.6 dB
8 users	2.2 dB	2.2 dB

5.2.3 Partial knowledge of the interference

In the previous section we saw that having ideal knowledge of the interference for the different modulation units leads to considerable performance gains. It is easy to see that this is a highly idealised scenario as having a perfect estimation of the interference for each sub-carrier of each OFDM symbol is not practically achievable. A more realistic scenario would be to assume that for each OFDM symbol duration we manage to obtain one estimate of the interfering power per sub-band, that is per block of 47 consecutive sub-carriers.

In order to quantify the improvement resulting from such an estimation method, simulations were run using the same configuration as in the previous section, but this time the LLRs are weighted using the band-averaged interfering power. The block error rates for QPSK and 16-QAM are in Figures 5.12 and 5.13 respectively. As one could expect, using the band-average leads to a lower performance gain than with per-carrier ideal estimation. Nevertheless, regardless of whether QPSK or 16-QAM modulation is used, weighting the LLRs with the band-averaged interference power leads to a noticeable performance gain.

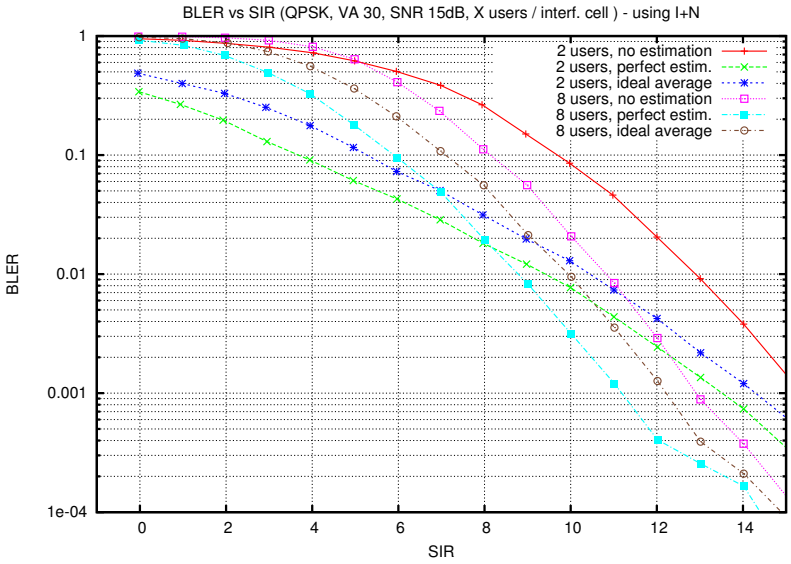

Figure 5.12: BLER for QPSK : band-averaged ideal interference estimation

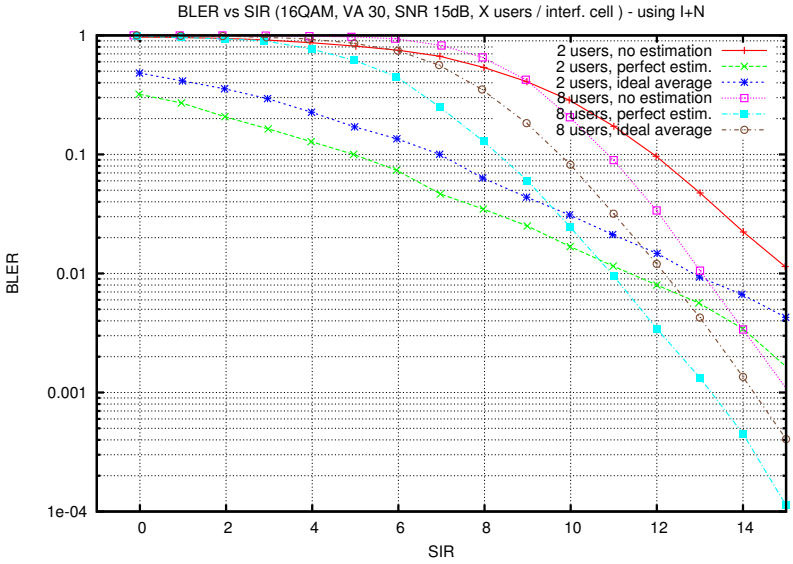

Figure 5.13: BLER for 16-QAM : band-averaged ideal interference estimation

The following table summarises the performance gain over no estimation for a BLER of 10^{-2} in the different configurations.

users per interfering cell	QPSK	16-QAM
2 users	2.4 dB	2.4 dB
5 users	1.4 dB	1.3 dB
8 users	1.0 dB	1.0 dB

5.3 Interferer location

In this section we focus on the interference estimation method that was described in section 4.2.2. This method tries to iteratively determine the allocation pattern, the number of users and the power of the interfering cells from measurements performed in the time-frequency units where the cell of interest does not transmit anything. For such time-frequency units to exist, the cell of interest cannot run at full load, so we consider a load of 8 users in this cell. Furthermore, we consider that the cell of interest and the interfering cells are synchronised both in time and in frequency.

5.3.1 Single interfering cell

Since the estimation algorithm works by iteratively detecting the interfering cells, we start by running a set of simulations with a single interfering cell loaded with either 5 or 8 users. The results when the interfering cell has 5 users are plotted in Figure 5.14 and those for 8 users are plotted in Figure 5.15.

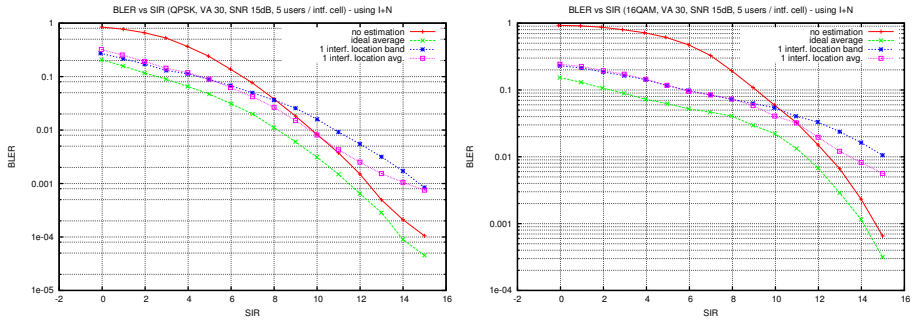

(a) QPSK

(b) 16-QAM

Figure 5.14: BLER for 5 users in a single interfering cell : interferer location

When 5 users are present in the interfering cell, we can see that for low SIR values, the interference estimation leads to a performance gain over no estimation at all. However, once the SIR reaches approximately 8dB for QPSK or 10dB for 16-QAM, interference estimation starts to fail and it actually decreases the system's performance. When 8 users are present in the interfering cell, we observe the same kind of behaviour, interference estimation improves the BLER for low SIR values but deteriorates it once the SIR reaches 4dB for QPSK or 7dB for 16-QAM. It is interesting to note that in

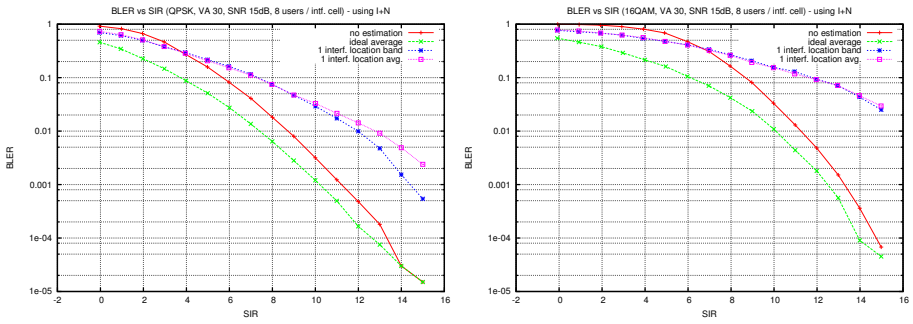

(a) QPSK

(b) 16-QAM

Figure 5.15: BLER for 8 users in a single interfering cell : interferer location

the region where interference estimation leads to a gain, there is no noticeable difference between using one power estimation per sub-band and using an averaged power estimation over all the sub-bands.

The poor performance at high SIR values can be explained by the fact that as the interference level drops, it becomes more and more difficult to distinguish the interference from the thermal noise, which leads to an erroneous detection of the interfering cells. It was to be expected that the algorithm would perform better when there are 5 users in the interfering cell than when there are 8, since in the first case the interference is concentrated on fewer time-frequency units and is therefore easier to pick up.

5.3.2 Two interfering cells

In this section we add an extra interfering cell to examine how the interferer location algorithm performs in a truly multicellular environment. The two interfering cells have relative powers of 0 and -5dB. The cell of interest still has a load of 8 users and we consider loads of 2, 5 or 8 users per interfering cell. The result for these three scenarios are respectively plotted in Figures 5.16, 5.17 and 5.18. The interferer location algorithm works by iteratively detecting the strongest interfering cells, so it is interesting to assess the influence of the maximum number of iterations. To this end, we try both detecting only the strongest interfering cell and detecting both interfering cells.

In Figure 5.16 we see that when 2 users are present in each interfering cell, the interferer location algorithm leads to a considerable performance gain over no estimation for low SIR values. As in the single interfering cell scenario, there is a cutoff SIR value (10 dB for QPSK, 12 dB for 16-QAM) above which it is better not to perform interference estimation. We can also see that the second iteration, that is to say the location of the weaker interfering cell, leads to an additional performance gain up to a certain SIR value (9dB for QPSK and 8dB for 16-QAM). Above this value, it is better not to perform the second iteration. This is not surprising considering that the second iteration makes its decisions based on the interference powers remaining after the first iteration. As the results of the first iteration become less reliable when the SIR increases, when the first iteration incorrectly locates the strongest interfering the second iteration makes a decision based on faulty metrics, leading to a further deterioration.

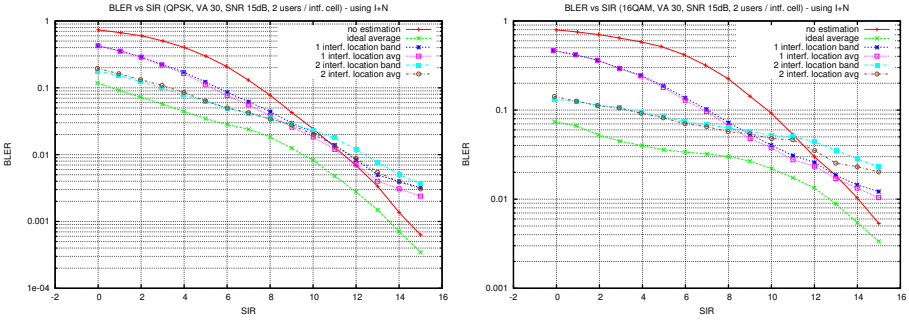

(a) QPSK (b) 16-QAM

Figure 5.16: BLER for 2 users per interfering cell : interferer location

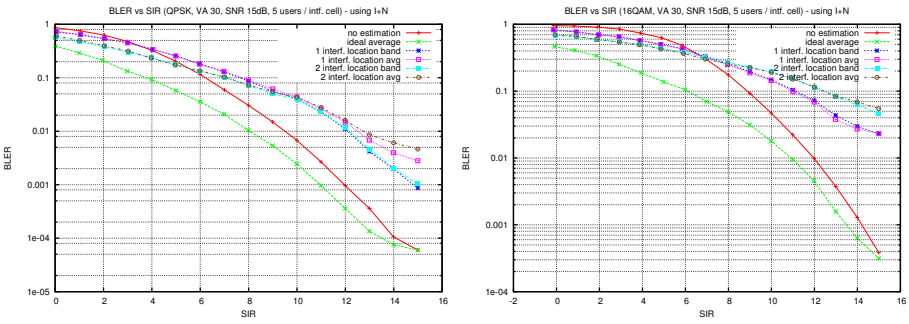

(a) QPSK (b) 16-QAM

Figure 5.17: BLER for 5 users per interfering cell : interferer location

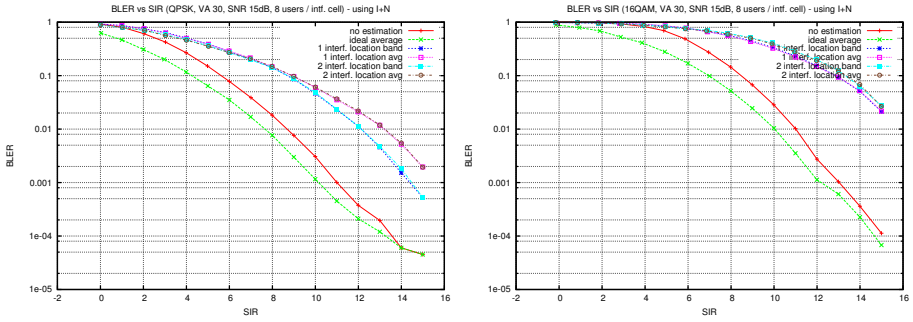

(a) QPSK

(b) 16-QAM

Figure 5.18: BLER for 8 users per interfering cell : interferer location

In Figure 5.17 we see that for 5 users per interfering cell, the performance of the iterative algorithm drops considerably and that above an SIR of 5dB for QPSK or 7dB for 16-QAM there is no gain over no estimation at all. A closer inspection reveals that while the allocation pattern set and number of users in the interfering cells are correctly estimated most of the time, the power estimate becomes highly unreliable. In figure 5.18 we see that the interferer location algorithm fails altogether when we consider 8 users per interfering cells and systematically leads to a decrease in performance.

In conclusion, we can say that the interferer location algorithm leads to performance gains only under certain conditions. The interfering cells need to be synchronised with the cell of interest and the loads of the interfering cells should not exceed 5 users. Furthermore, at high SIR values it is better not to perform the interference estimation. It is not altogether surprising that such conditions are required for the algorithm to work. We are operating on a frequency selective fading channel, so different sub-carriers experience different fadings. It is therefore difficult to predict the interference level in the time-frequency units of interest (the T-F units where the cell of interest is active) based on observations in the interference-only cells.

5.4 Demapping-remapping

It was illustrated in the previous section that locating the interfering cells is difficult to achieve in a multi cell environment. In this section, results based on the simple estimation method describe in section 4.2.3 are presented. For these simulations, the cell of interest is at full load, meaning it has 15 active users. Furthermore, we no longer consider that the cell of interest and the interfering cells are synchronised in time.

5.4.1 Raw demapping-remapping

At first set of simulations was run in which the LLRs are weighted directly with the difference between the received signal and the result of the demapping-remapping operation. Loads of 2, 5 or 8 users were considered for the interfering cells, but for the sake of clarity only the results for 2 and 8 users are presented. In these simulations, we

examine both QPSK modulation (Figure 5.19) and 16-QAM modulation (Figure 5.20).

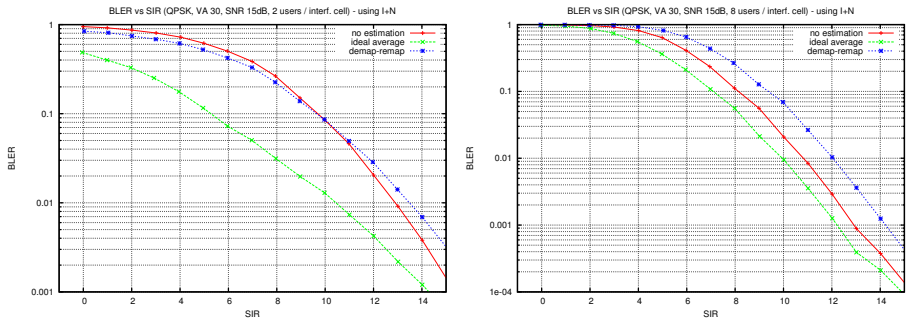

Figure 5.19: BLER for QPSK : raw demapping-remapping estimation

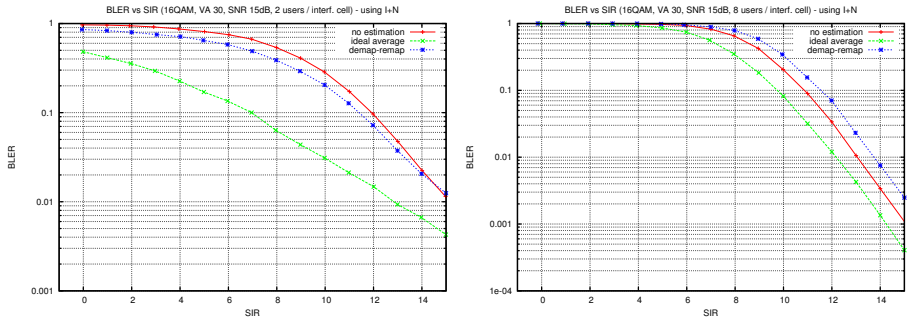

Figure 5.20: BLER for 16-QAM : raw demapping-remapping estimation

The results for 2 users per interfering cell show that for high interfering powers, using the raw demapping-remapping estimation method leads to a slight improvement over no estimation at all, but once the SIR reaches a certain level (10dB for QPSK and 15dB for 16-QAM) it is better not to perform any estimation at all. When there are 8 users per interfering cells the results are even worse, nothing is gained by using the demapping-remapping method.

These results are not surprising since the metric we considered is not a reliable estimate of the interference on a symbol per symbol basis. If the interference is strong for a given symbol interval, the demapping operation followed by a hard decision can lead to choosing the wrong constellation point as the transmitted signal, which in turn gives a false estimate of the interference power. Furthermore, from an information theory point of view, we are using any new information. We are in fact using the same information twice, once in the interference estimation for a hard decision and a second time in the channel decoder for a soft decision.

5.4.2 Applying filtering

We saw in the previous section that using the demapping-remapping estimate of the interference power directly is not an efficient estimation method as it leads at best to a

poor performance improvement and in some cases actually deteriorates performance. In this section, some filtering is applied to the interference estimate in order to exploit the fact there is a strong correlation between the interference experienced in adjacent sub-carriers. The filtering that is applied is a simple polynomial interpolation, either of order zero (averaging) or of order one. This filtering is applied per sub-band, that is to say per block of 47 consecutive sub-carriers of a given OFDM symbol.

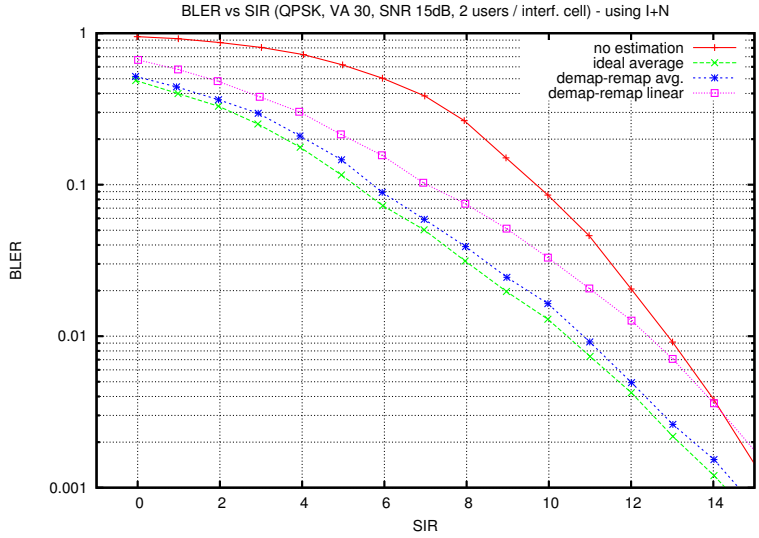

Figure 5.21: BLER for QPSK, 2 users per interfering cell : filtered demap-remap

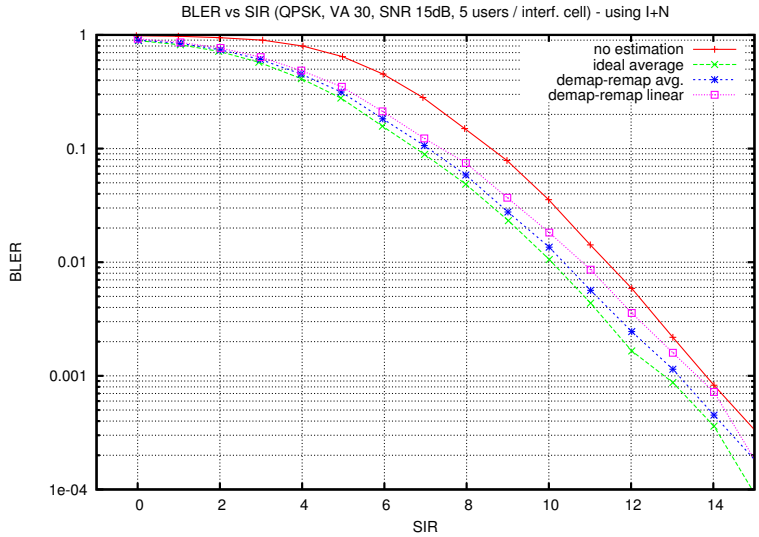

Figure 5.22: BLER for QPSK, 5 users per interfering cell : filtered demap-remap

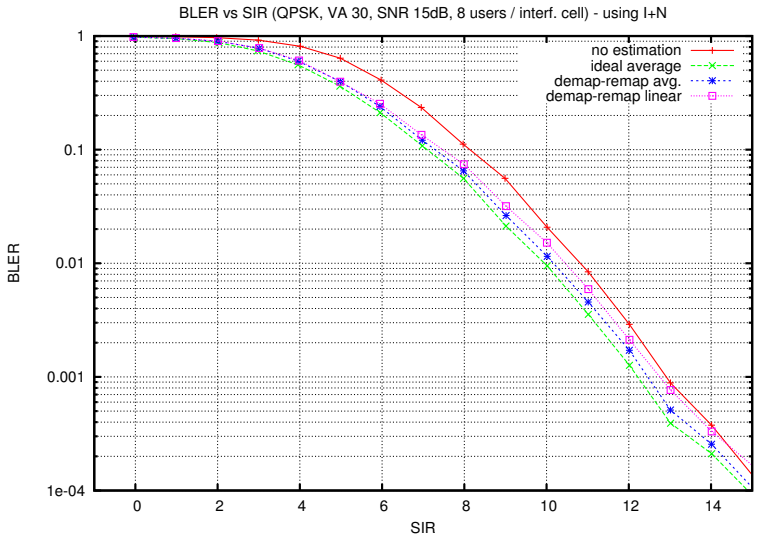

Figure 5.23: BLER for QPSK, 8 users per interfering cell : filtered demap-remap

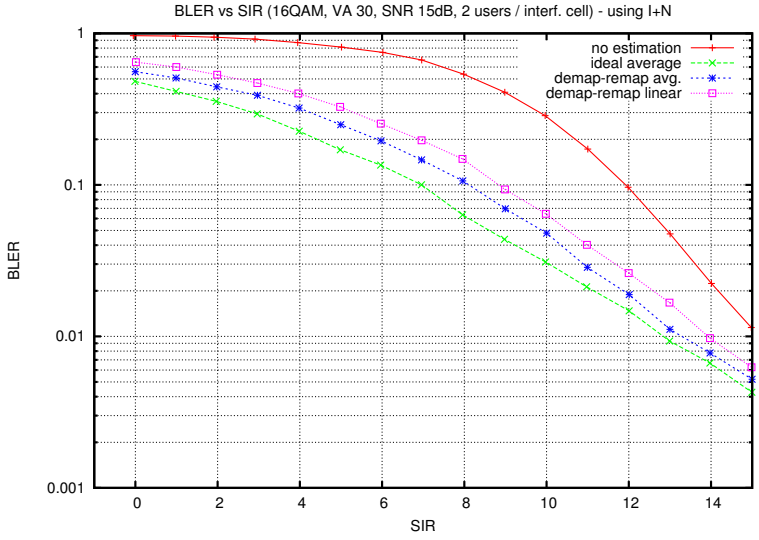

Figure 5.24: BLER for 16-QAM, 2 users per interfering cell : filtered demap-remap

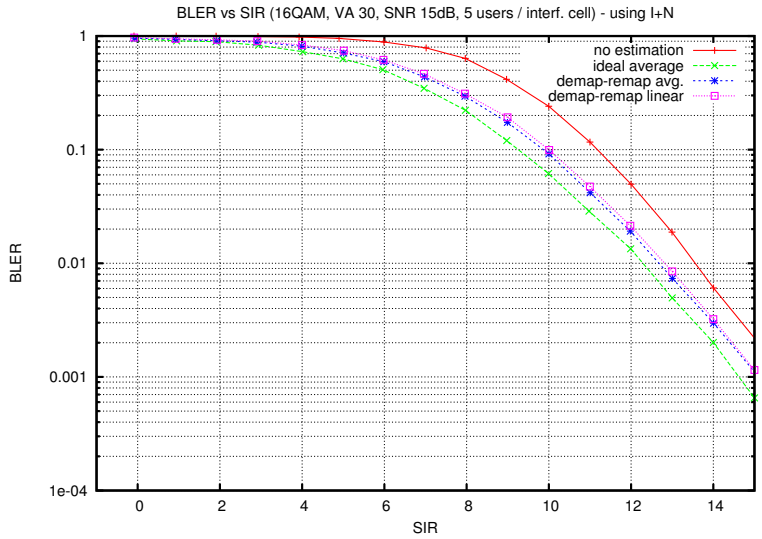

Figure 5.25: BLER for 16-QAM, 5 users per interfering cell : filtered demap-remap

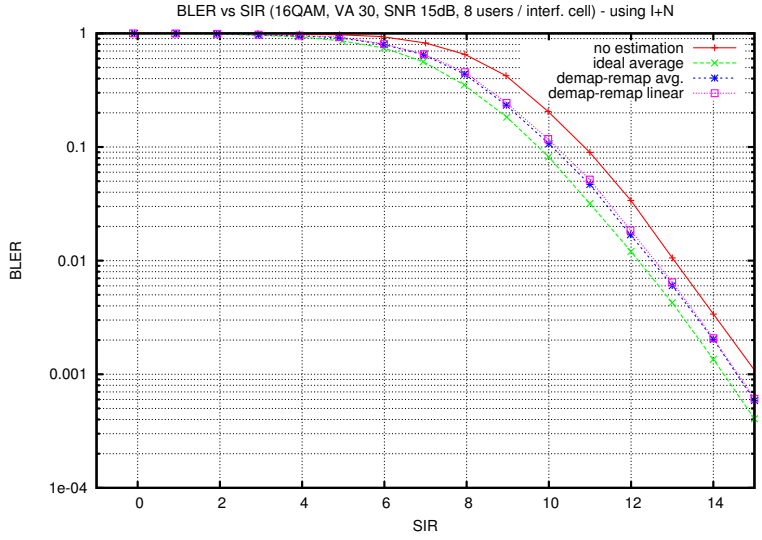

Figure 5.26: BLER for 16-QAM, 8 users per interfering cell : filtered demap-remap

The results for QPSK are plotted in Figures 5.21, 5.22 and 5.23, those for 16-QAM are plotted in Figures 5.24, 5.25 and 5.26. It is apparent from these plots that applying filtering considerably improves the interference estimate obtained by the demapping-remapping method.

For all of the configurations we examined, using the band-averaged demapping-remapping interference estimate leads to significant performance gains over no estimation. In all of the configurations, the performance when weighting the LLRs with the band-averaged estimate tracks the performance of band-averaged ideal estimation with a near-constant offset. This offset is of approximately 0.5dB, except for 16-QAM at 2 users per interfering cell, in which case it is closer to 1dB. The following table summarises the performance gain of band-averaged demapping-remapping over no estimation for a BLER of 10^{-2} in the different configurations.

users per interfering cell	QPSK	16-QAM
2 users	2.1 dB	1.9 dB
5 users	1.1 dB	0.9 dB
8 users	0.7 dB	0.6 dB

A slightly surprising result is that the polynomial interpolation of order one yields a performance which is less than that of the interpolation of order zero. One possible explanation is that the interference estimate resulting from the demapping-remapping operation is very noisy so that increasing the order of the interpolation does not smooth this estimate enough.

In conclusion, we can say that weighting the LLRs passed to the channel decoder using the demapping-remapping estimation method followed by averaging for each sub-band is a very interesting means of increasing the system's performance. Not only does it yield performance gains regardless of the type of modulation, the load of the interfering cells and the SIR level, but it does so at the cost of very little computational complexity.

5.5 Using an equivalent SNR mapping

In the previous sections, we evaluated the performance of various estimation methods when the LLRs are weighted according to equation 4.4. In this section, we try to determine whether weighting the LLRs using an (SIR,SNR) to equivalent SNR mapping can lead to additional performance gains.

5.5.1 AWGN channel

The mapping we consider was developed based on measurements for uncoded transmissions over an AWGN channel, so a first test is to evaluate how this mapping performs on an AWGN channel. In order to separate the influence of the LLRs adjustment method from the actual interference estimation method, we use either the ideal knowledge of the interference presented in section 5.2.2 or a the ideal band-average presented in section 5.2.3. Two unsynchronised interfering cells were considered, with loads of 2, 5 or 8 users. However, as the results for these different loads had the same characteristics, only the results for 8 users in the interfering cells are presented in Figure 5.27.

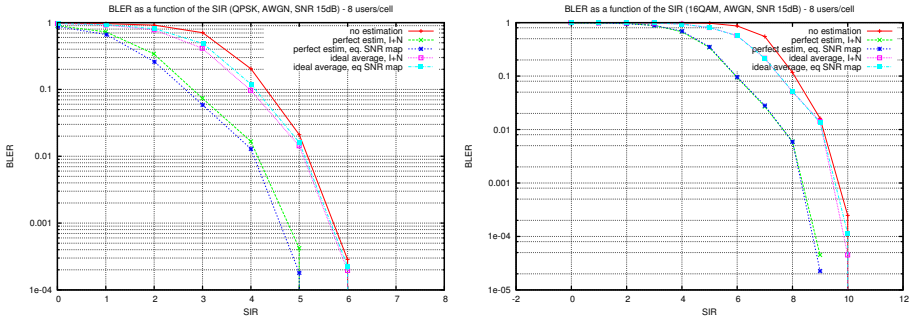

Figure 5.27: BLER for 8 users per interf. cell, AWGN : equivalent SNR mapping

As we can see, for QPSK modulation weighting the LLRs using our equivalent SNR mapping leads to a slight gain (approximately 0.2dB) in the case of ideal knowledge of the interference. However, when using the ideal band-average estimation, the equivalent SNR mapping actually causes a slight decrease in performance. For 16-QAM modulation, there is no noticeable difference between using the SNR mapping and the simple $I+N$ weighting. This is not very surprising considering that in section 3.1.2 we showed that for uncoded 16-QAM, interference and noise of equal powers have the same impact on the bit error rate.

5.5.2 Vehicular A 30km/h channel

In Figure 5.28 we plotted the results obtained when using the equivalent SNR mapping for an ITU Vehicular A 30km/h channel. It is apparent from these plots that both for QPSK and for 16-QAM modulation, using the equivalent SNR mapping leads to a slight decrease in performance over the simple $I+N$ weighting. As in the AWGN case, 16-QAM is less affected than QPSK.

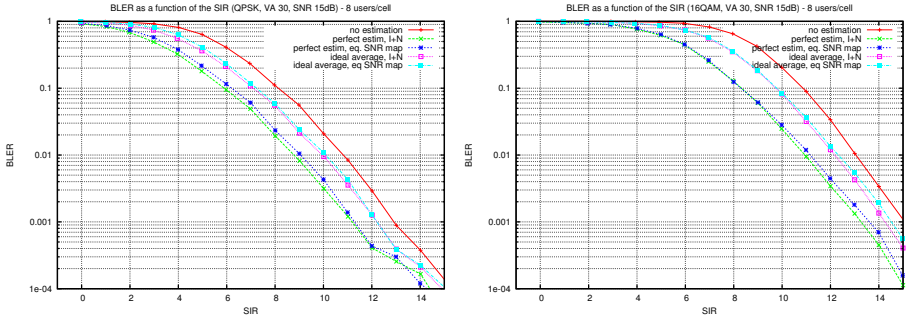

Figure 5.28: BLER for 8 users per interf. cell, VA 30 : equivalent SNR mapping

In conclusion, equivalent SNR mapping fails to improve the performance of the system on a realistic fading channel. Nevertheless, these results are interesting as they show that two weighting methods which are quite different in nature still lead to very similar results.

This page intentionally contains only this sentence.

Chapter 6

Conclusions and future work

6.1 Conclusions

From the various simulations that were run, it is obvious that frequency-hopping OFDMA is a multiple access technique that is robust to multicellular interference. Furthermore, since the inter-cell interference that is experienced in an OFDMA system is not homogeneous, it is possible to reduce its impact by estimating the time-frequency distribution of the interference. In this case, the impact of interference is lower than a homogeneous additive white Gaussian noise of the same average power.

It is usually assumed that when dealing with interference it is best to average it out over the modulation symbols; this is the behaviour of CDMA. In FH-OFDMA, the interference is averaged out at the block level, but the interference is still heterogeneous at the modulation symbol level, which can be exploited to improve the performance of the system performance. This gain is not just theoretical, it can be achieved in practical situations since we designed a low complexity interference estimation algorithm and validated its performance by means of realistic simulations.

6.2 Future work

6.2.1 Improving the interference estimates

In section 5.4.2, we evaluated the demapping-remapping interference estimation method presented in section 4.2.3 and saw that provided some filtering is applied, the resulting estimate of the interference can be used to weight the log-likelihood ratios passed to the channel decoder to achieve substantial performance gains with little computational complexity.

The filtering that was applied operates on the sub-bands of each OFDM symbol. If the cell of interest and the interfering cells were synchronised both in time and in frequency, this would be a very logical choice since the user traffic multiplexing scheme that is used operates on sub-bands, and hence the interference level would be approximately constant in each sub-band. However, when time synchronisation is not assumed, this is no longer true and applying filtering on a per sub-band basis is arbitrary. It would be interesting to study the effect of using a low-pass filter on the interference estimate for a whole OFDM symbol.

It should also be noted that the demapping-remapping interference estimation is

based on a hard-decision and is by nature a non-linear operation. It would be interesting to investigate the effect of applying non-linear filtering techniques to the interference estimate thus produced.

6.2.2 Improving the LLR weighting

The log-likelihood ratio weighting methods that were developed in section 4.1.3 are based on the assumption that we can obtain a good approximation of the true LLR by multiplying the metric produced by the demapper by a function of the instantaneous SIR and SNR. Simulations confirmed that using such an LLR weighting leads to a performance gain. In order to produce a better approximation of the true LLR, it would be necessary to also take into account the actual value of the metric output by the demapper when performing the weighting. It is very likely that such an improved LLR weighting would lead to further performance gains.

Bibliography

[1] D. Ramakrishna, N. B. Mandayam, R. D. Yates, "Subspace-Based SIR Estimation for CDMA Cellular Systems", *IEEE Trans. Veh. Technology, vol. 49, no. 5, Sep. 2000.*

[2] 3GPP, "Feasibility Study for OFDM for UTRAN Enhancement", 3GPP TSG RAN WG1, TR 25.892.

[3] Huawei, "Link-level OFDM performances under realistic inter-cell interference", *3GPP TSG RAN WG1, Tdoc R1-031171, meeting #35, Lisbon, Portugal, November 17-21, 2003.*

[4] Huawei, "New results on realistic OFDM interference", *3GPP TSG RAN WG1, Tdoc R1-040189, meeting #36, Malaga, Spain, February 16-20, 2004.*

[5] A. Sampath, and D. R. Jeske, "Analysis of Signal-to-Interference Ratio Estimation Methods for Wireless Communications Systems".

[6] M. L. McCloud, L. L. Scharf, "Interference Estimation with Applications to Blind Multiple-Access Communications Over Fading Channels", *IEEE Trans. Inform. Theory, vol. 46, no. 3, May 2000.*

[7] B. Sklar, "A Primer on Turbo Code Concepts", *IEEE Commun. Mag., vol. 35, no. 12, pp 94-101, Dec. 1997.*

[8] 3GPP, "High Speed Downlink Packet Access (HSDPA); Overall Description", *TS 25.308 V5.2.0, March 2002*.

[9] 3GPP, "High Speed Downlink Packet Access (HSDPA); Physical Layer Aspects", *TR 25.950 V5.0.0, March 2002.*

[10] S.W. Golomb, H.Taylor, "Construction and Properties of Costas Arrays", *Proceedings of the IEEE, vol. 72, no. 9, pp. 1143-1163, Sep. 1984.*

[11] M. Malkowski, C. C. J. Chua, G. Vivier, D. Imbeni, O. Seller, J. Lainé, A. Kemper, D. Callonnec, "Spectrum Efficient Multicast and Asymetric Services in UMTS including Performance Simulation Results", *IST-20001-35125/OverDRiVE/WP1/D15, April 2004*

This page intentionally contains only this sentence.

TRITA—S3—RST—0409
ISSN 1400—9137
ISRN KTH/RST/R--04/09--SE

Radio Communication Systems Lab.
Dept. of Signals, Sensors and Systems
Royal Institute of Technology
S–100 44 STOCKHOLM
SWEDEN

JEREMY LAINÉ Interference Estimation in a Multicellular OFDMA Environment